



Ciência e Tecnologia de Alimentos

ISSN: 0101-2061

revista@sbcta.org.br

Sociedade Brasileira de Ciência e
Tecnologia de Alimentos
Brasil

DÍAZ, Rodrigo Emilio; ACUÑA, Sergio Miguel; SEGURA, Luis Andrés
Construction of 2D transparent micromodels in polyester resin with porosity similar to
carrots

Ciência e Tecnologia de Alimentos, vol. 31, núm. 4, outubro-diciembre, 2011, pp. 960-966

Sociedade Brasileira de Ciência e Tecnologia de Alimentos
Campinas, Brasil

Available in: <http://www.redalyc.org/articulo.oa?id=395940111022>

- How to cite
- Complete issue
- More information about this article
- Journal's homepage in redalyc.org

redalyc.org

Scientific Information System

Network of Scientific Journals from Latin America, the Caribbean, Spain and Portugal

Non-profit academic project, developed under the open access initiative

Construction of 2D transparent micromodels in polyester resin with porosity similar to carrots

Construção de micro modelos 2D transparentes em resina de poliéster com porosidade similar a das cenouras

Rodrigo Emilio DÍAZ¹, Sergio Miguel ACUÑA¹, Luis Andrés SEGURA^{1*}

Abstract

Microscopic visualization, especially in transparent micromodels, can provide valuable information to understand the transport phenomena at pore scale in different process occurring in porous materials (food, timber, soils, etc.). Micromodels studies focus mainly on the observation of multi-phase flow, which presents a greater proximity to reality. The aim of this study was to study the process of flexography and its application in the manufacture of polyester resin transparent micromodels and its application to carrots. Materials used to implement a flexo station for micromodels construction were thermoregulated water bath, exposure chamber to UV light, photosensitive substance (photopolymer), RTV silicone polyester resin, and glass plates. In this paper, data on size distribution of a particular kind of carrot we used, and a transparent micromodel with square cross-section as well as a Log-normal pore size distribution with pore radii ranging from 10 to 110 μm (average of 22 μm and micromodel size of 10 \times 10 cm) were built. Finally, it stresses that it has successfully implemented the protocol processing 2D polyester resin transparent micromodels.

Keywords: flexography; transparent micromodels; porous materials.

Resumo

Visualização microscópica, especialmente em micromodelos transparente, pode fornecer informações valiosas para a compreensão dos fenômenos de transporte de poros em diferentes processos que ocorrem em materiais porosos (alimentos, madeira, solos, etc.). Micromodelos estudos centram-se principalmente na observação de fluxo multifásico, que apresenta uma maior proximidade com a realidade. O objetivo deste trabalho foi estudar o processo de flexografia e sua aplicação na fabricação de resina de poliéster micromodelos transparente e sua aplicação para as cenouras. Os materiais utilizados para implementar uma estação de flexo para fazer micromodelos fosse um banho termostaticado, câmara de exposição à luz ultravioleta, a substância fotossensível (fotopolímero), resina de poliéster, silicone RTV e placas de vidro. No presente trabalho foram utilizados dados sobre a distribuição do tamanho de um tipo particular de cenoura e foi construído um micromodelo transparente, com secção transversal quadrada, tamanho e distribuição log-normal de poros com raios de poros que variam de 10-110 μm (média de 22 μm e micromodelo tamanho de 10 \times 10 cm). Por fim, salienta que implementou com sucesso o processamento do protocolo 2D micromodelos resina de poliéster transparente.

Palavras-chave: flexografia; micromodelos transparente; materiais porosos.

1 Introduction

Microscopic visualization can provide valuable information for understanding the transport phenomena at the pore scale. Transparent micromodels reproduce porous media, either natural or synthetic, which in turn can be used to simulate transport processes at the pore scale. These micromodels are defined as networks of pores that capture the complexity of porous materials either natural or artificial see (BUCKLEY, 1991) for more extensive review of the topic.

In the specialized literature, there are various types of classification of pore sizes (macro, meso, and micropores). Another classification of pore size is based on their size and function in the porous matrix; the so-called “pore bodies” refers to the larger pores, and the “pore throats” refers to the smaller pores connecting adjacent pore bodies that are responsible for the transport properties of the porous matrix.

Micromodels applications are diverse distinguishing the high energy micromodels (silicon or glass) and low energy micromodels (resins). However, regardless of their energy, they show us the interfacial motion of fluids allowing differentiating between varieties of transport mechanisms that have a similar behavior to other phenomena. In recent times, there has been a great effort to understand the importance of pore geometry and topology, fluid properties, and interaction of capillary forces and gravity to determine the displacement paths of two fluid phases. The construction of the first low surface energy micromodel was made by Bonnet and Lenormand (1977), who used a molding technique to build a micromodel using a photopolymer plate (Dicril 152). This technique has advantages from the point of view of surface energy because being a low-energy, visualizations are unaffected by capillary effects, and on the other hand, the pores cuts are straight when compared with

Received 13/4/2010

Accepted 4/9/2010 (004793)

¹ Departamento de Ingeniería en Alimentos, Universidad del Bío-Bío, Casilla, 447, Chillán, Chile, e-mail: lsegura@ubiobio.cl

* Corresponding author

those made of glass. Recently, based on the technique developed by Chatzis (1982), Zamorano (2007) developed transparent glass micromodels with a very good resolution. Oyarzún and Segura (2009) built glass micromodels that capture the main features of biological materials, particularly wood. These authors constructed transparent 2D glass micromodels that represent the wood anatomy using statistical information on the sizes of cells (pores), geometric forms thereof, the thickness of the cell wall, and the connections between cells (throats). Drying experiments with interesting results related to the transport mechanisms involved in this kind of materials were performed using these micromodels.

Similarly the work developed by Oyarzún and Segura (2009), it is possible to develop micromodels based on other types of biological materials. Hence, firstly we need to know statistics of the sizes of pores of such materials. In this regard, it is important to mention the study conducted by Karathanos, Kanellopoulos and Belessiotis (1996), who characterized porous structures of several foods such as apples, carrots, and potatoes using the technique of mercury porosimetry and helium pycnometry. Through the data provided by Karathanos, Kanellopoulos and Belessiotis (1996), it is possible to simulate a network of pores that have similar characteristics to the studied materials (apple, carrot, and potato), and then to apply lithography techniques to generate transparent micromodels representing them. This would provide a permanent model, as well as repetitive and reproducible testing at any time for the research development.

The micromodels development, either glass or resin, are based on the so-called flexography technique. This is one of the printing techniques used in packaging materials including corrugated cartons, polymer films (polyethylene, polypropylene, polyester, etc.), printing napkins, toilet paper, paperboard folding, newspapers, etc. In the present study, the process of flexography and its application in the manufacture of polyester resin transparent micromodels using patterns generated from statistical data of the carrot porosity was studied.

2 Materials and methods

The following materials were used in the micromodels construction: polyester resin, cobalt, hydrogen peroxide, Silicone RTV-3325, paraffin wax, Silica Gel, carbon tetrachloride, liquid Photopolymer (Exell), ethanol, commercial soda plate glass (110 × 110 × 4 mm), acetone, and glass and plastic material.

Additionally, the following equipment was used: a flexo station consisting of an electric oven (model Nex TO-16) adapted with a fan inside, an ultraviolet light projection camera, and a thermoregulated water bath. A Dremel Multipurpose, an optical microscope (Nikon Eclipse E200), a digital camera (Nikon Coolpix 990), and a digital meter walk (VWR grade 2) were also used.

For the manufacture of the polyester resin micromodels, the first step was to obtain the photopolymer plate mold. The procedure steps are summarized as follows: The liquid photopolymer was poured into a glass plate with the dimension of the micromodel, and the photopolymer was covered with the pattern (negative) of a porous system before being exposed to ultraviolet light. Next, the photopolymer which did not reacted

with ultraviolet light was removed using a solvent developer. This solvent developer selectively dissolves the areas that were not exposed to ultraviolet light, leaving a porous structure embossed in the photopolymer material. Using the RTV silicone, the mold was removed from the structure. Thereafter, the mold was filled with polyester resin, the intergranular spaces were filled with paraffin wax, the micromodel was sealed with polyester resin, and the paraffin wax was removed from the micromodel by applying temperature.

Figure 1 shows a schematic representation of the process developed by Bonnet and Lenormand (1977) and adapted to this work. An important variation of the technique developed by these authors was the incorporation of a liquid photopolymer, hence reducing significantly the depth of the pores obtained. The protocol for the manufacture of micromodels used in the present study work is detailed as follow:

2.1 Conditioning of glass plates

Glass plates were buffed with sandpaper (400 grit sandpaper to water) to remove sharp edges, being careful not to leave scratches on the surface. Next, they were immersed in a solution containing 2% of detergent.

The glass plates were cleared on both sides with a cotton swab and rinsed with abundant running water to remove residual detergent.

The plates were then washed with distilled water to remove residual salts present in drinking water. The plates were immediately transferred to an oven, where they were dried for 30 minutes at 150 °C. To avoid contamination of the plate surfaces, they were attached with metal clips, which were held to the oven rack.

2.2 Preparation of photopolymer container frame

In order to pour the liquid photopolymer into the glass plate, an adhesive tape was placed (like a frame) to delimit the glass plate surface, into where the photopolymer would be poured. This corresponds to the photopolymer etching area. The depth of pore or throat was given by the thickness of the tape used (DÍAZ, 2009).

2.3 Filling the frame with photopolymer

Photopolymer at ambient temperature showed a very high viscosity, which caused problems in filling frame due to the formation of occlusions. Hence, it was necessary to reduce its viscosity increasing temperature. After conditioning the photopolymer, the framework was filled with a syringe. This was done in a zigzag pattern. Therefore, it was necessary to cut a sheet of transparency that was used as a protective film and served as a support for the pattern recorded in the photopolymer. Finally, the frame was sealed with a glass plate (DÍAZ, 2009).

2.4 Patterns design

It was created a series of two-dimensional micromodel patterns from a code in Visual Basic (v6) that generates pore size distributions. The code was fed with statistical values from the selected materials, i.e., mean, standard deviation, maximum

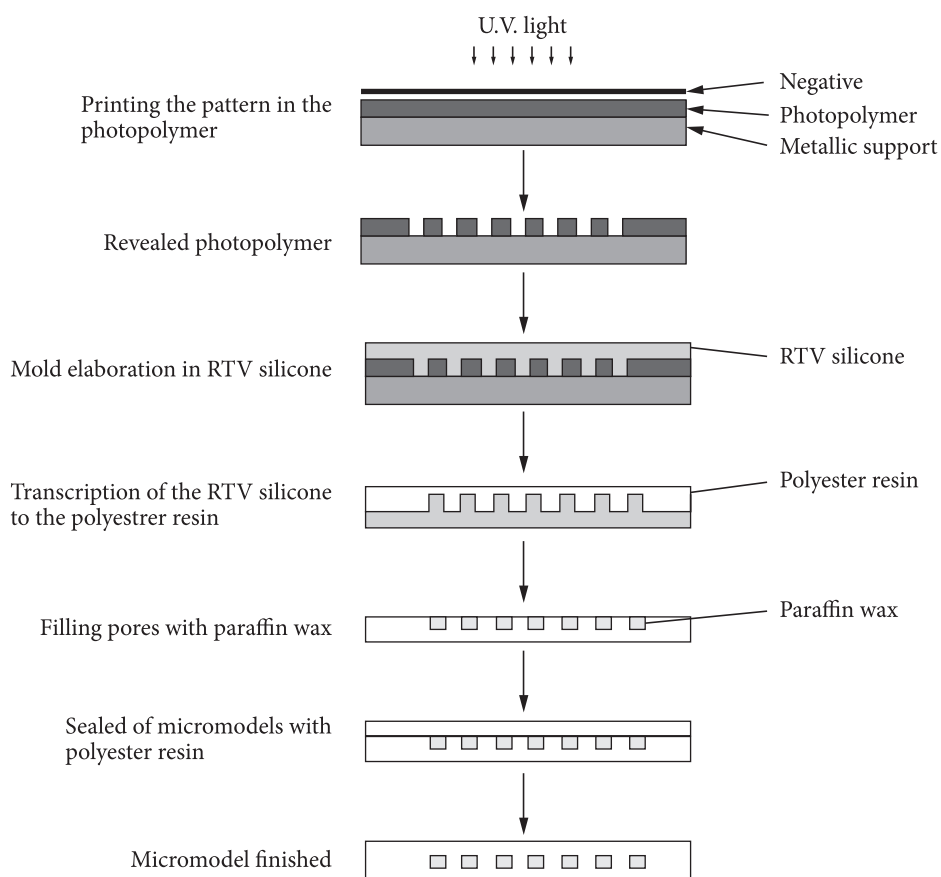


Figure 1. Scheme of the technique developed by Bonnet and Lenormand (1977) and adapted to this work.

and minimum radius, and number of pores of desired material according to the procedure described by Oyarzún (2008).

Once the data from the distribution of pore size and shape were generated, they were drawn in the Autocad software (version 16.1, Autodesk Inc.). Figure 2a shows a pattern generated of 50×50 pores with throats radii distributed according to a Log-Normal function distribution type, in which the pore throats (channels) are represented in black. In Figure 2b, a pattern of 100×100 pores with the same distribution function type is shown.

In order to obtain micromodels able to capture the geometrical and topological main features of foodstuffs, a methodology to obtain a carrot pattern was developed.

Data obtained by Karathanos, Kanellopoulos and Belessiotis (1996) were used to design the inner cell array of carrots. For this type of material, the authors present a bimodal pore size distribution, shown in Figure 3. In this Figure, there are two peaks of pore size, which raises the question of whether pores are uniformly distributed (large pores coexisting with small pores) or there are two well defined zones with different pore sizes, one of them with larger pores and the other with smaller pores. Additionally, it is necessary to consider that the mercury porosimetry technique is a procedure that when run, will deform matrix pores, which can affect the results.

As mentioned previously in the present study, Karathanos and co-workers' data were verified using carrots micrographs

obtained by Scanning Electron Microscopy (SEM). From these micrographs, it was determined that the bimodal distribution obtained by Karathanos, Kanellopoulos and Belessiotis (1996) was due to the fact that pores with a smaller size distribution were located in a narrow radial zone of the carrots' cross-sectional area separating two different zones containing larger pores, i.e., the groups with the smaller pores were located near the central area, and the other groups (with larger pores) were located in the center and outside of the cross-sectional area of the carrots' samples.

With the information obtained from Karathanos, Kanellopoulos and Belessiotis (1996), a computer-generated pattern of the porous structure for pores radii with a pore size distribution greater than $10 \mu\text{m}$ was printed on a transparent film (slide). Figure 3b,c, show the pattern obtained for the carrot cells, which subsequently was used in the construction of a micromodel. As shown in Figure 3, the square-shaped pores are completely different from the image of the carrot; however this does not affect transport properties since the radius of the throats is more important for them because of the pore radius control the transport properties of the material.

2.5 Exposure to ultraviolet light

Once the desired pattern was made, it was aligned, covered with glass plate to close the frame, and the photopolymer was then exposed to the ultraviolet light for a period of 5 minutes and 10 seconds (OYARZÚN; SEGURA, 2009).

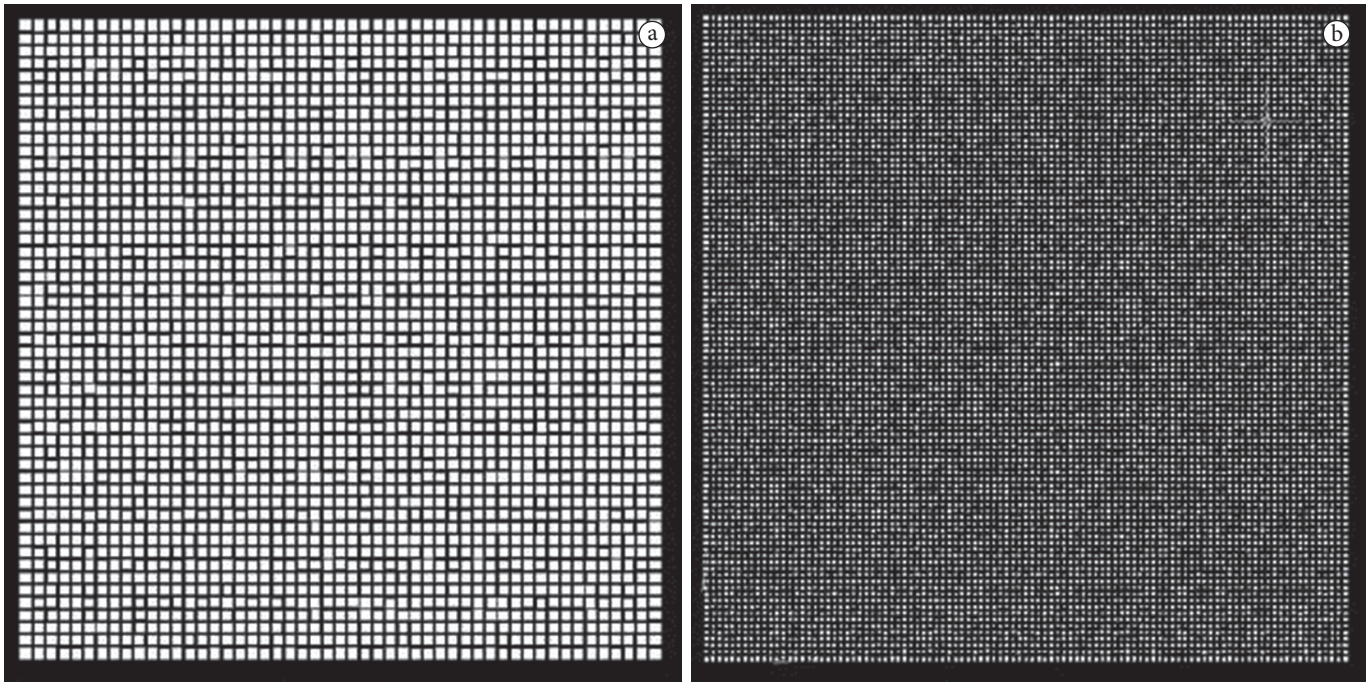


Figure 2. a) 50×50 pores pattern, node-to node distance of 2 mm, and throat radius of Log-Normal type between 200 and 400 μm . b) 100×100 pores pattern, node-to-node distance of 1 mm, and throat radius of Log-Normal type between 200 and 300 μm .

2.6 Rinse and removal of surplus

The plates recently exposed to ultraviolet light were dipped in detergent solution at 10% v/v and the unreacted photopolymer was removed mechanically by a brush and rinsed with abundant distilled water.

After rinsed, the plates were taken to an oven for 30 minutes at a temperature of 80 °C and were post-exposed to UV light for a period of 10 minutes (DÍAZ, 2009).

2.7 RTV mold

Thereafter, the sides of the photopolymer developed (pattern) were framed with a 2 mm thick rubber sheet. Next, the RTV silicone was put inside the framework, which was used to extract the mold pattern obtained from the photopolymer. The RTV silicone was used according to manufacturer's specifications; this is a two component material: a base and a catalyst that was added by 5% by volume and the reaction time was 24 hours at room temperature (DÍAZ, 2009).

2.8 Micromodel part one

The RTV silicone mold obtained in the previous step was framed with a smooth rubber of 2 mm and filled with the polyester resin prepared according to manufacturer's specifications. Next, the frame was covered with a glass plate. The polyester resin was poured into the frame at an angle of 45°. The complete polyester resin reaction occurred at 48 hours, and the polyester resin was then demoulded. After this, the polyester resin mould was introduced in the oven at 80 °C for 6 minutes; finally, the RTV mold was extracted using a knife to obtain the "micromodel part one", which is the first stage of the micromodel building process (DÍAZ, 2009).

2.9 Filling the pores and throats with paraffin wax

The imprinted plate was then filled with paraffin wax. For this, a piece of paraffin wax was rubbed in the pattern obtained in the micromodel part one stage to fill all pores and throats. The excess of paraffin wax was removed to leave the surface smooth, and the surface was finally sanded with 180 and 400 grit sandpapers (DÍAZ, 2009).

2.10 Sealing micromodel

Once the pores and throats were filled with paraffin wax, the smooth side of micromodel obtained in "the micromodel part one" stage was again covered with adhesive tape and framed with a smooth rubber of 2 mm. The polyester resin was poured into the frame at an angle of 45°. The complete polyester resin reaction occurred at 48 hours. After the reaction was complete, the micromodel was demoulded. This procedure was similar to that described in the micromodel part one section (DÍAZ, 2009).

2.11 Modeling the geometry of micromodel

Once the micromodel was removed from the glass plate, the desired geometric shape of the micromodel was obtained. This procedure was obtained by a cutter grinder (Dremel) using the blade at 10,000 rpm. (DÍAZ, 2009).

2.12 Extraction of paraffin wax

The extraction of paraffin wax from the micromodel was done by the diluting with carbon tetrachloride (CCl_4). The sealed micromodel was put into a container filled with carbon tetrachloride, and when the paraffin wax was completely dissolved, the solution was extracted from the micromodel (DÍAZ, 2009).

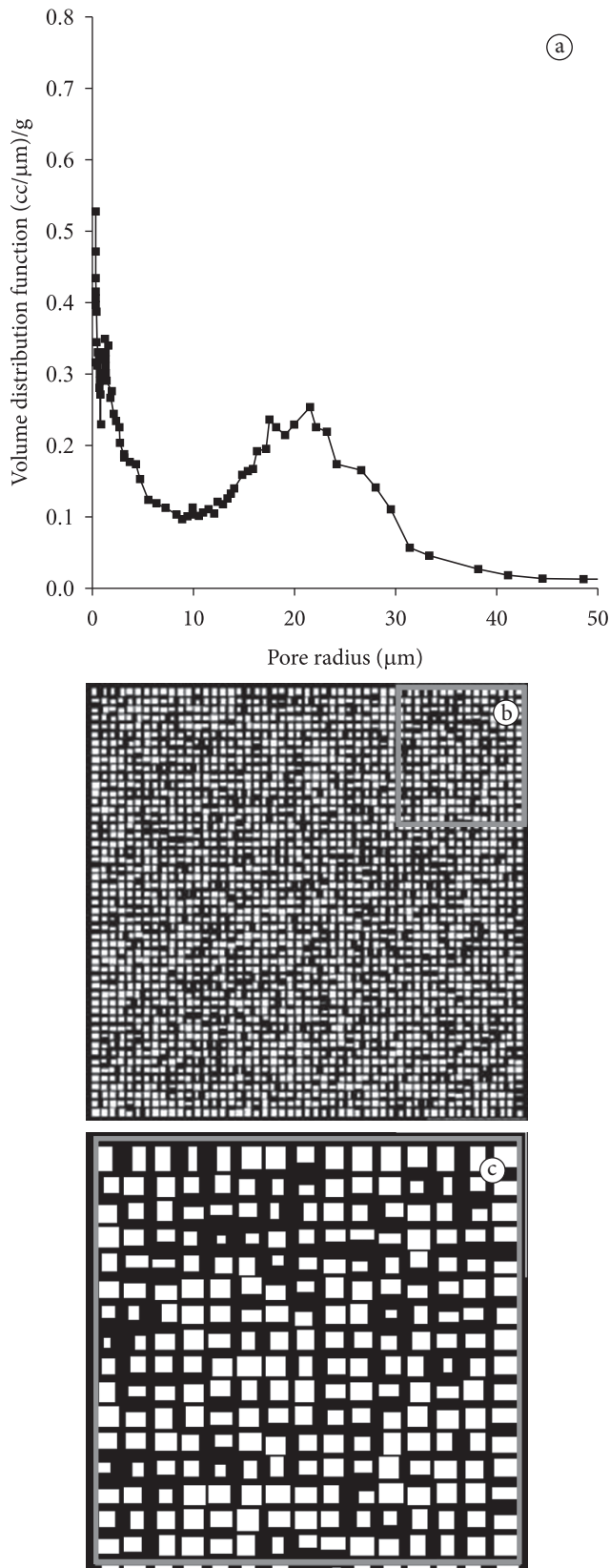


Figure 3. a) Pore size distribution of carrot determined by mercury porosimetry (KARATHANOS; KANELLOPOULOS; BELESSIOTIS, 1996); b) Bidimensional pattern of carrot cells, general view, 10 × 10 cm; c) larger view.

3 Results and discussion

From the micromodels building protocol developed in the present study, resin micromodels were elaborated with a minimum throat radius of 100 μm . Moreover, the pore cuts of the resulting channels (pore throats) were straight compared with those made by glass. On the other hand, the shapes of the channels obtained in the present work were well-defined for a node-to-node distance higher than 1 mm. More importantly, a reduction of the 90% in the throat depth was achieved comparing the micromodels manufactured by Bonnet and Lenormand (1977) with the ones obtained in the present work. The throat depth of the micromodels obtained in the present study was 0.1 mm. The pore throats shapes were well-defined for channels with a node-to-node distance higher than 1.5 mm. There was deformation of the porous matrix for shorter distances resulting in pores, which were initially square, with a round geometry. The pores were deformed for channels with a node-to-node distance lower than 1.5 mm such as those obtained by these authors. In general, the results of the present work were better than those obtained by Bonnet and Lenormand (1977).

From a subroutine in Visual Basic (Version 6) and from available statistical data of a given porous material (maximum and minimum throat radii, mean and standard deviation), pore size distributions and networks images were generated using the Autocad software. With these results, the micromodels were built according the implemented protocol. Figure 4 shows a micromodel with a uniform pore distribution generated by this procedure. In order to illustrate the usefulness of such tools, a micromodel obtained was filled with a volatile liquid and dried at room temperature. Figure 4 shows a micromodel that was flooded with a given liquid (carbon tetrachloride) and then dried horizontally (without gravity effects). The dark color in the image (Figure 4) corresponds to the zones that have not been dried and therefore are liquid-filled zones, while light areas correspond to the zones where the liquid has been evaporated

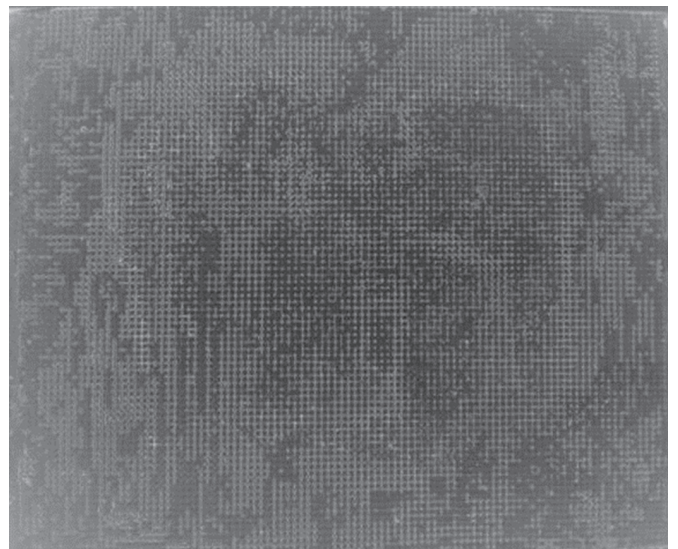


Figure 4. 100 × 125 Pores micromodel, node-to node distance of 1.5 mm, and 5 minutes and 10 seconds exposure time. Plate dimension are 12.5 × 15.5 cm. White zone: gas; dark zone: liquid.

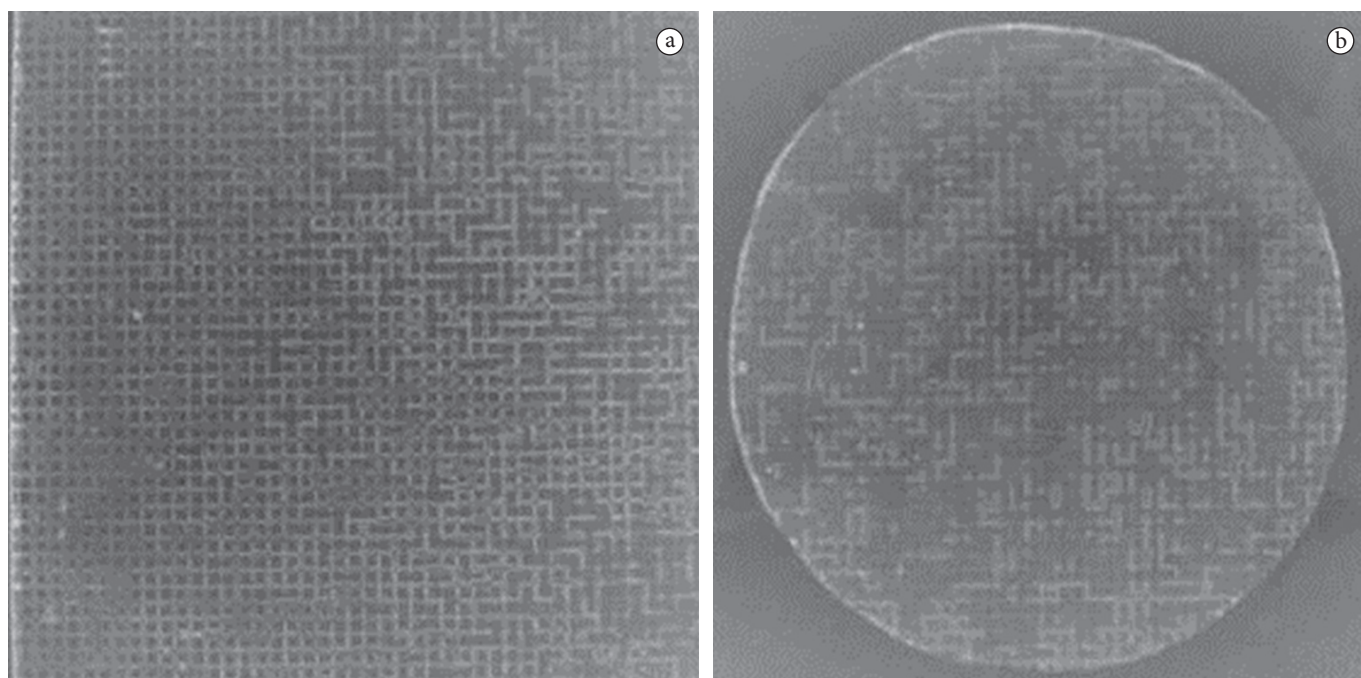


Figure 5. Carrot micromodels of pore size distribution: a) 45×45 pores square micromodel, 9×9 cm plate dimension; b) circular micromodel of 8.5 cm diameter.

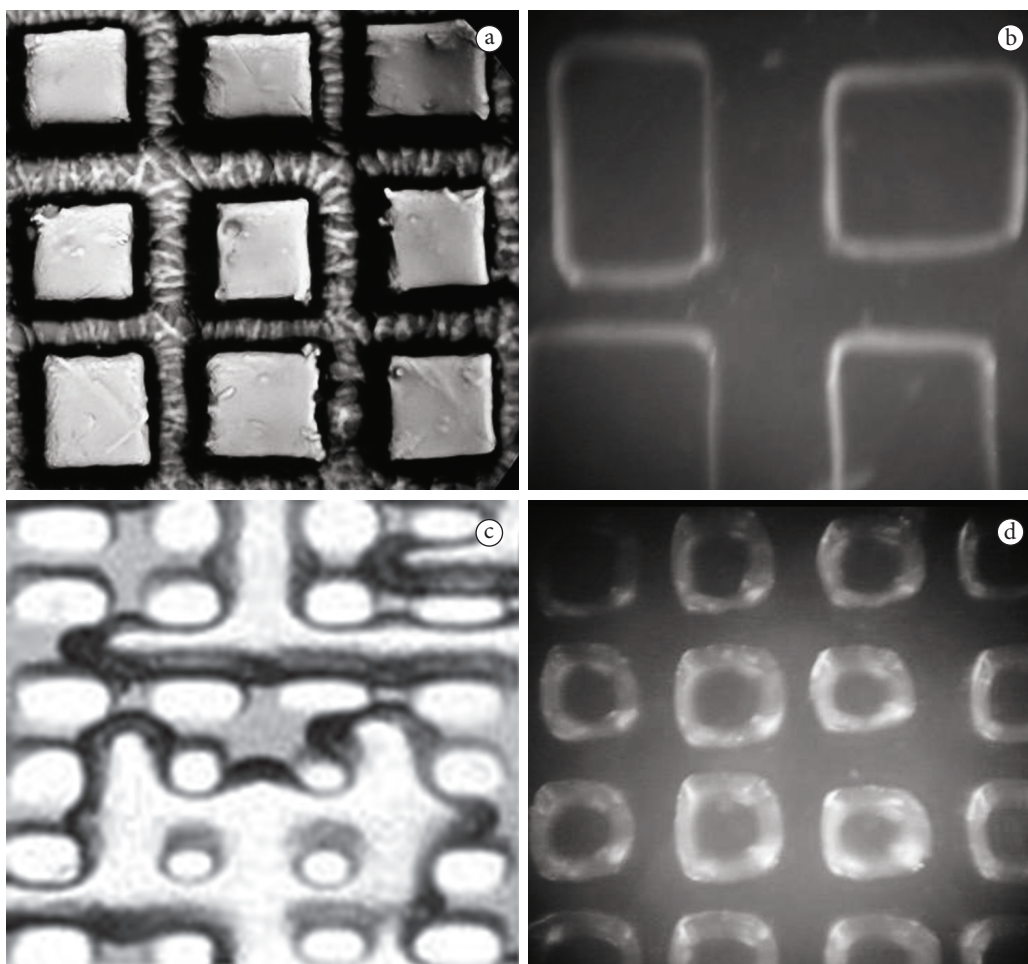


Figure 6. a) Glass micromodel (ZAMORANO, 2007); b, d) polyester resin micromodels elaborated in this work; c) micromodel elaborated by Bonnet and Lenormand (1977).

(dried), the air-filled zones. In this image, it can be observed the heterogeneity of the porous matrix. The subroutine in Visual Basic (Version 6) was fed with the available carrots' statistical data such as the maximum and minimum radii, mean value, and standard deviation of the pore size distribution obtained by Karathanos, Kanellopoulos and Belessiotis (1996). Then the obtained data were exported to the Autocad software. The image obtained using the Autocad software represented the carrot pore structure. Next, from these results, a micromodel was built according the implemented protocol (Figure 5). The Micromodels in Figure 5 represent porous structures with a Log-Normal pore size distribution with a node-to-node distance of 2 mm. The geometrical shape was the difference between both micromodels: the first one was square and the other was circular. Both micromodels were exposed to ultraviolet light for a time of 5:10 (minutes:seconds). Finally, the micromodels were flooded with carbon tetrachloride and then dried horizontally (without gravity effects) at normal ambient conditions. The liquid phase is represented by the dark color and the gas phase by light zones (air).

Figure 6 shows images of the different micromodels in order to compare the results obtained with others available in the specialized literature. Figure 6a shows a glass micromodel obtained by Zamorano (2007), while Figure 6b shows a resin micromodel obtained in the present study. By comparing these images, it is possible to see that the glass micromodel has irregular channels produced by acid attack, unlike the resin micromodels which shows that the channels have straight cuts and smooth surfaces. Similarly, Figure 6c shows a resin micromodel elaborated by Bonnet and Lenormand (1977), and Figure 6d a resin micromodel obtained in the present work. Figure 6c shows pores and throats partially flooded by liquid and gas, while Figure 6d shows a dried section of the micromodel built in this work. Both images have the same node-to-node distance, but the micromodels obtained in the present study have a 90% reduction in the throats depth compared with ones obtained by Bonnet and Lenormand (1977). In addition, the matrix definition was improved because the micromodels pattern obtained in the present work have a square configuration, while those obtained by Bonnet and Lenormand (1977) had an almost completely circular shape. Moreover, from Figure 6b, it is possible to see that the matrix definition obtained in the present study was better than that obtained by Bonnet and Lenormand (1977); however, it should be noted that this was because the node-to-node distance was 1.5 mm.

Finally, in the specialized literature we can find some experimental evidence related to the use of this kind of micromodels, specifically the isothermal drying experiments. On their experiments and simulations, Laurindo and Prat (1996, 1998) used a 2D polyester resin micromodel. Specifically, a 140×140 network containing about 39,000 ducts (pore throats) with seven classes of width (from 100 to 600 μm) distributed at random using a Log-Normal distribution. Tsimpanogiannis et al. (1999) used a 2D glass micromodel, in which the pore body/throat thickness were spatially distributed following a Rayleigh pore size distribution with an average pore throat radius of 450 μm and mean pore body radius of 900 μm .

4 Conclusions

A protocol to obtain 2D polyester resin micromodels based on the protocol developed by Bonnet and Lenormand (1977) was implemented. The Micromodels obtained have the following characteristics: straight cuts of the solid matrix, low surface energy, and a reduction in the throats depth of 90% compared with those built by Bonnet and Lenormand (1977). Additionally, micromodels that capture the main features of carrots were obtained. It is also possible to extend this use to other natural materials of practical interest. Accordingly, it is necessary to emphasize the wide range of applications of these kind of micromodels, specifically to study different mechanisms of fluid transport (liquids and gases) that occurs at microscopic scale in different processes or unit operations present not only in the food industry, but also in the chemical industry and in transport processes associated with soils among others.

Acknowledgements

The authors are grateful for the financial support provided by the CONICYT-Chile through the project FONDECYT n° 11060081.

References

- BONNET, J.; LENORMAND, R. Realisation de micromodels pour l'étude des écoulements polyphasiques en milieu poreux. *Revue de l'Institut français du pétrole*, v. 42, p. 477-480, 1977.
- BUCKLEY, J.S. Multiphase Displacement in Micromodels. In: MORROW, N. R. (Ed.). *Interfacial phenomena in petroleum recovery*. New York: Marcel Dekker Inc.; 1991. p. 157-189.
- CHATZIS, I. *Photofabrication technique of 2-D glass micromodels*. New Mexico: Petroleum Recovery Research Center, 1982. p. 1-6. PRRC Report 82-12.
- DÍAZ, R.E. *Protocolo para la elaboración de micromodelos transparentes 2D en resina de poliéster*. 2009. 72f. Tesis (Graduación em Ingeniero Alimentos)-Universidad del Bío, Chillán, 2007.
- KARATHANOS, V.; KANELLOPOULOS, N.; BELESSIOTIS, V. Development of Porous Structure During Air Drying of Agricultural Plant Products. *Journal of Food Engineering*, v. 29, p. 169-183, 1996. [http://dx.doi.org/10.1016/0260-8774\(95\)00058-5](http://dx.doi.org/10.1016/0260-8774(95)00058-5)
- LAURINDO, J. B.; PRAT, M. Numerical and experimental network study of evaporation in capillary porous media. Phase Distributions. *Chemical Engineering Science*, v. 51, n. 23, p. 5171-5185, 1996.
- LAURINDO, J. B.; PRAT, M. Numerical and experimental network study of evaporation in capillary porous media. Drying rates. *Chemical Engineering Science*, v. 53, n. 12, p. 2257-2269, 1998. [http://dx.doi.org/10.1016/S0009-2509\(97\)00348-5](http://dx.doi.org/10.1016/S0009-2509(97)00348-5)
- OYARZÚN C. *Distribución de Fluidos y Transporte de Humedad a Escala de Segmentos de Poro Durante el Secado Isothermal de Madera*. Chile, 2008. Tesis (Magister en Ciencia y Tecnología de la Madera)-Universidad del Bío, Concepción, 2008.
- OYARZÚN, C. A.; SEGURA, L.A. Design and construction of glass micromodels for the study of moisture transport in woods. *Drying Technology*, v. 27, p. 14-29, 2009. <http://dx.doi.org/10.1080/07373930802565731>
- TSIMPANOIANNIS, I. N. et al. Scaling theory of drying in porous media. *Physical Review E*, v. 59, n. 4, p. 4353-4365, 1999. <http://dx.doi.org/10.1103/PhysRevE.59.4353>
- ZAMORANO C. *Protocolo para la elaboración de Micromodelos Transparentes 2D en vidrio*. 2007. Tesis (Graduación em Ingeniero Alimentos)-Universidad del Bío, Chillán, 2007.